Magnetic and Galvanomagnetic Properties of Intermettallic Compounds Er_<1-x>Y_xFe_2 in Cubic Laves Phase

Bulletin of the College of Science
University of the Ryukyus No. 47 : 1 −21 (1989)

Magnetic and Galvanomagnetic Properties of Intermetallic Compounds $Er_{1-x}Y_xFe_2$ in Cubic Laves Phase

Yowa KADENA, Shigeki MUTOH* and Katsuma YAGASAKI
Department of Physics, College of Science,
University of the Ryukyus, Nishihara, Okinawa, 903−01, Japan
(Received 17 Nov., 1988)

Magnetization, electrical resistivity and the Hall resistivity have been measured on polycrystalline $Er_{1-x}Y_xFe_2$ in cubic Laves phase. All the compounds have been confirmed to be ferrimagnetic except for YFe_2 which is ferromagnetic.

Curie temperature T_c decreases slightly with increasing x. They have a compensation temperature θ_c at which the spontaneous magnetization has a minimum.

The magnetic properties are discussed on the basis of the molecular field theory and the electrical resistivity and the Hall constants are discussed on the basis of the localized moment model.

§ 1. Introduction

In rare earth metals, $4f$ electrons, which are responsible for their magnetic properties, are deep inside the closed orbitals. Their magnetic properties are explained in terms of the localized moment models. On the other hand, the magnetic electrons in iron group elements have

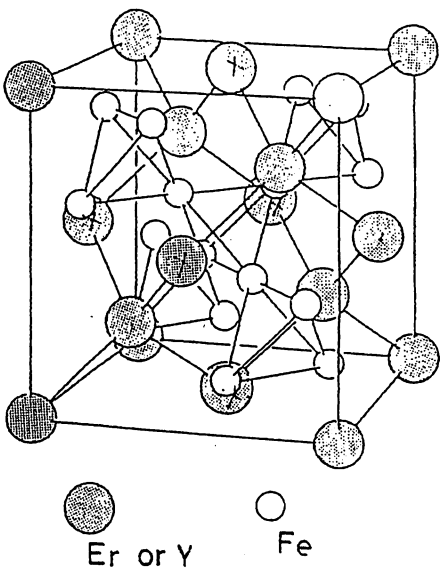

Fig.1; Crystal structure for the cubic Laves phase.

* Prsent adress: Japan Univac Soft Engineering, Babashitacho 1-1, Shinjuku, Tokyo 162, Japan

been explained by both the localized and itinerant models.

In our specimens, $Er_{1-x}Y_xFe_2$ a part of Er is replaced by nonmagnetic Y, which has orbitals similar to those of rare earth metals. The crystal structure of these speciments is $MgCu_2$ type cubic-Laves phase as shown in Fig.1. With these specimens, magnetic properties can be revealed without changing crystal structure and the state of conduction electrons. It is very interesting to investigate how the magnetic moment with different character cooperates with each other and what magnetic and galvanomagnetic character they have. We have measured the temperature dependence and also the concentration dependence of magnetic, electrical and galvanomagnetic properties of this system.

Results are discussed on the basis of the molecular field theory and the localized moment model.

§ 2. Experimental

a. Specimens

Purities of Er, Y and Fe metals were 99.9%. Rough materials with stoichiometric composition were melted and remelted several times in an argon jet furnace to get homogeneous compounds. Weight loss in the process of the melting was within 0.02%. Since $ErFe_2$ and YFe_2 are eutectic as shown in Fig.2, specimens were annealed for two weeks at 600° C to 1000° C to get stable Laves phase. Specimens were confirmed to be in a single phase of Laves phase by X-ray diffraction pattern analysis. $Er_{1-x}Y_xFe_2$ specimens were prepared for x=0.0, 0.3, 0.4, 0.5, 0.6 and 1.0.

b. Measurement

Magnetization, and the Hall constant measurements were performed over the temperature range from 77 to 600K. Electrical resistivity measurements were made over the temperature range from 77 to 800K. Liquid nitrogen was used for measurements in low temperature. High purity helium gas was introduced into specimen holder case as heat exchange atmosphere. Measurements were made in a vacuum at high temperatures. Multimeter and digital voltometer were connected to the NEC micro-computer PC-8801 to perform experiment automatically. AuFe-Chromel and Pt-Pt/Rh thermocouples were used for low and high temperature measurements, respectively.

Magnetization measurements were performed by using Faraday type magnetic balance in fields up to 15 kOe. Electrical resistivity measurements were made by means of a standard four-probe method. Electrical current was reversed for each measurement to prevent thermomotive force due to the possible temperature difference between electric probes.

Specimens were cut from the ingots, by using a crystal cutter, into parallelepipeds of $1\times 1\times 15mm^3$ for the electrical resistivity and $3\times 0.3\times 15mm^3$ for the Hall resistivity. They were annealed for two days to remove strains possibly introduced in the process of cutting. Copper wires of 50 and 150 micrometer diameter were used as the electric probes for low and high temperature measurements, respectively. Two-probe method was utilized for the Hall constant measurements. Temperature was controlled within 0.2K during the measurements. Electric current and magnetic field were reversed to get rid of the effects due to magneto-

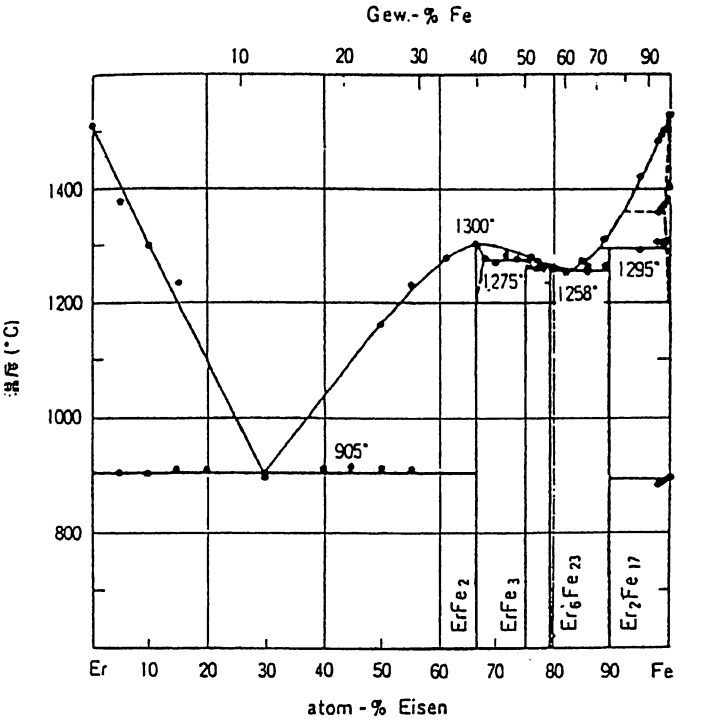

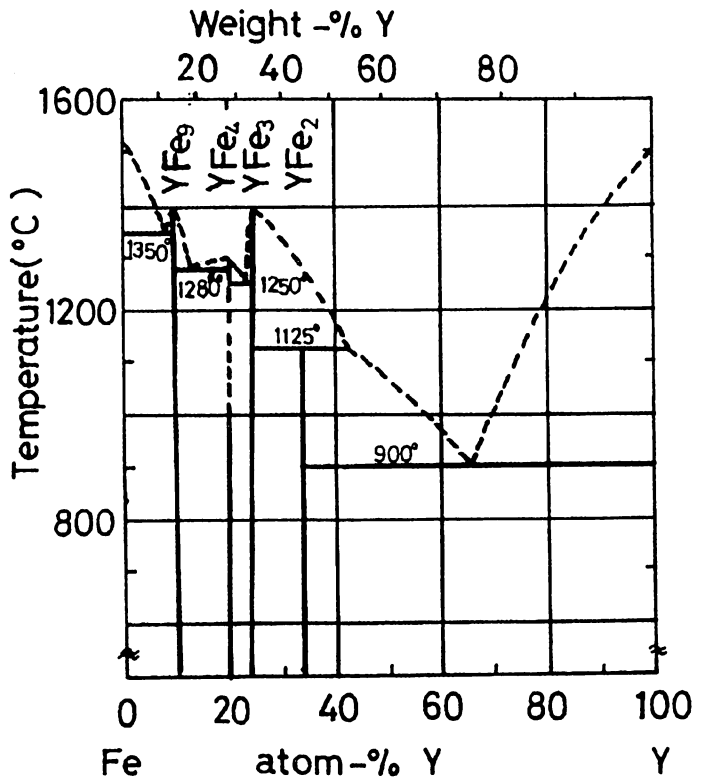

Fig.2; Metallurgical phase diagram for Fe-Y and Er-Fe alloys.

resistance and electro motive force. We obtained the Hall resistivity by averaging the four experimental values.

§ 3. Results

a. Lattice Constants

Fig.3 shows the x dependance of lattice constants at room temperature. Lattice constant increases linearly with increasing x. As the ionic radius of Y^{3+} is larger than that of Er^{3+}, these facts suggest that the rigid sphere model (Vegard's law) is valid in these compounds. Our results on $ErFe_2$ and YFe_2 agree with those of Buschow and Stapele[3] within 0.1%.

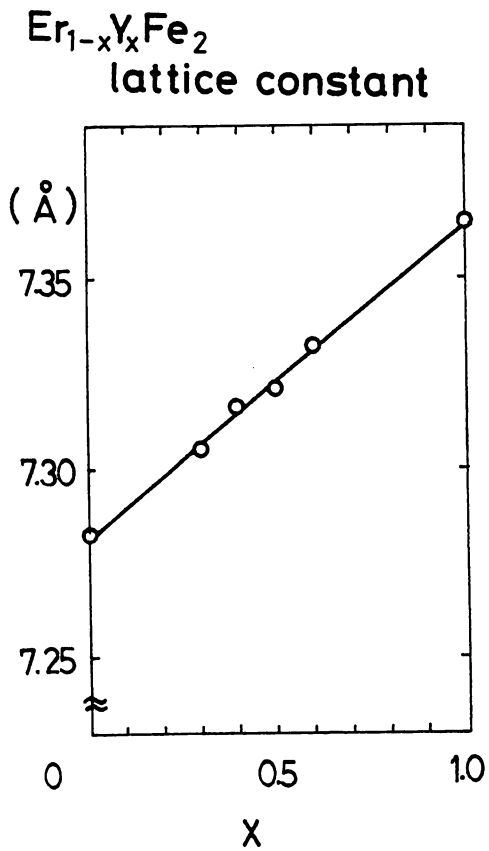

Fig.3; Lattice constant for $Er_{1-x}Y_xFe_2$.

b. Magnetization

Magnetization curves of $ErFe_2$ at temperatures 77 and 298K are shown in Fig.4. These curves indicate that $ErFe_2$ has a spontaneous magnetization. Temperature dependences of spontaneous magnetization are measured at fields 11 kOe, because magnetization saturates above 10 kOe for all the temperatures.

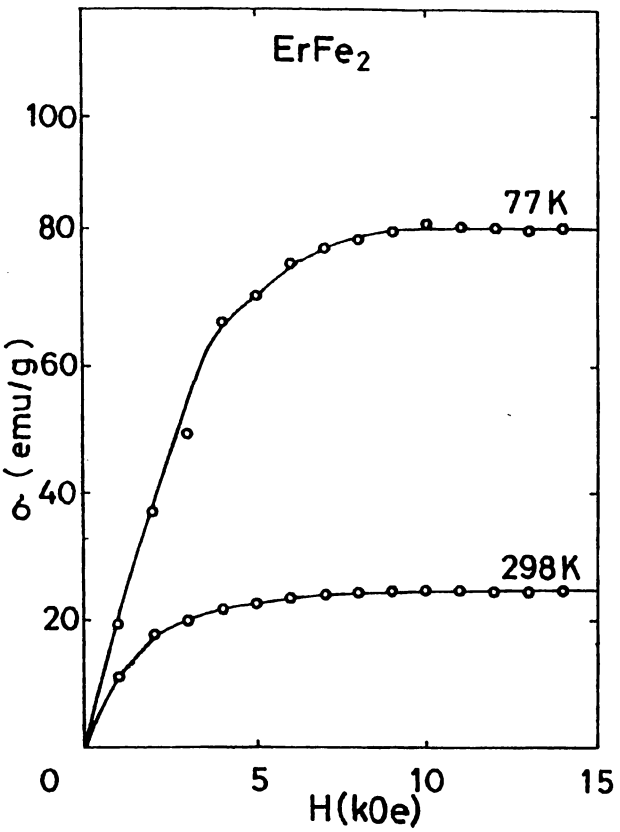

Fig.4; Magnetization curve for $ErFe_2$ at 77K and 298K.

In Fig.5, temperature dependence of magnetization is shown. Except for YFe_2, magnetization has a minimum at certain temperature. This fact means that the magnetic moments are devided into two parts and that one of the parts is antiparallel to the other part. Further, no minimum in YFe_2 means that this compound has only one sublattice moments. Thus we can conclude that ferromagnetic alignment of Er moments is antiparallel to the ferromagnetic alignment of Fe moments-that is ferrimagnetic-for all the compounds except for YFe_2 which is ferromagnetic. Compensation temperature (θ_c), at which magnetization has a minimum, decreases with increasing Y concentration. The Curie temperature (T_c), at which the spontaneous magnetization goes to zero, is about 570K for all the specimens.

In Fig.6, temperature dependences of T_c and θ_c are shown. T_c decreases slightly and linearly with increasing x, however, the compensation temperature θ_c, at which the magnetization becomes minimum, decreases with increasing x. Magnetic moments of Er and Fe at 0K are $9\,\mu_B$, and about $2\,\mu_B$, respectively.

We assume that the moment of Er decreases more quickly than that of Fe with increasing temperature. When the moment of Fe will become equal to that of Er at some temperature, the spontaneous magnetization of the system will be zero at this temperature. This is called as the compensation temperature θ_c. The fact that θ_c decreases with decreasing Er content supports the above assumption.

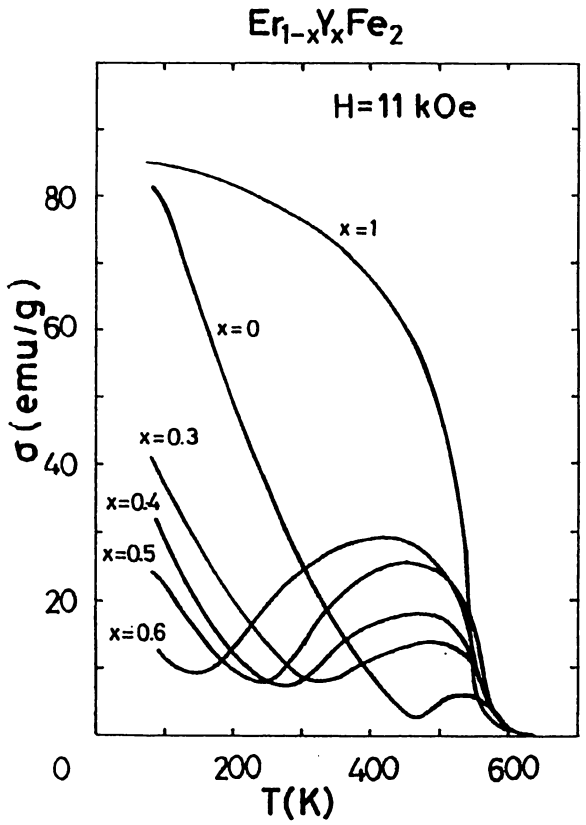

Fig.5; Temperature dependence of the magnetization at 11kOe for $Er_{1-x}Y_xFe_2$.

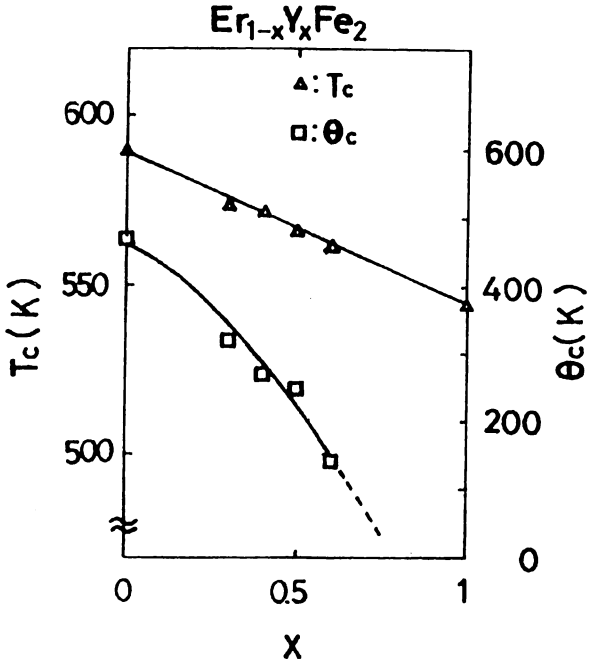

Fig.6; Curie temperature T_c and compensation temperature θ_c for $Er_{1-x}Y_xFe_2$.

c. Electrical resistivity

In Fig.7, temperature dependence of electrical resistivity is shown. There are knees at T_c, eventhough they are not so conspiquous as in the case of magnetization. Electrical resistivity at any temperature decreases as x increases.

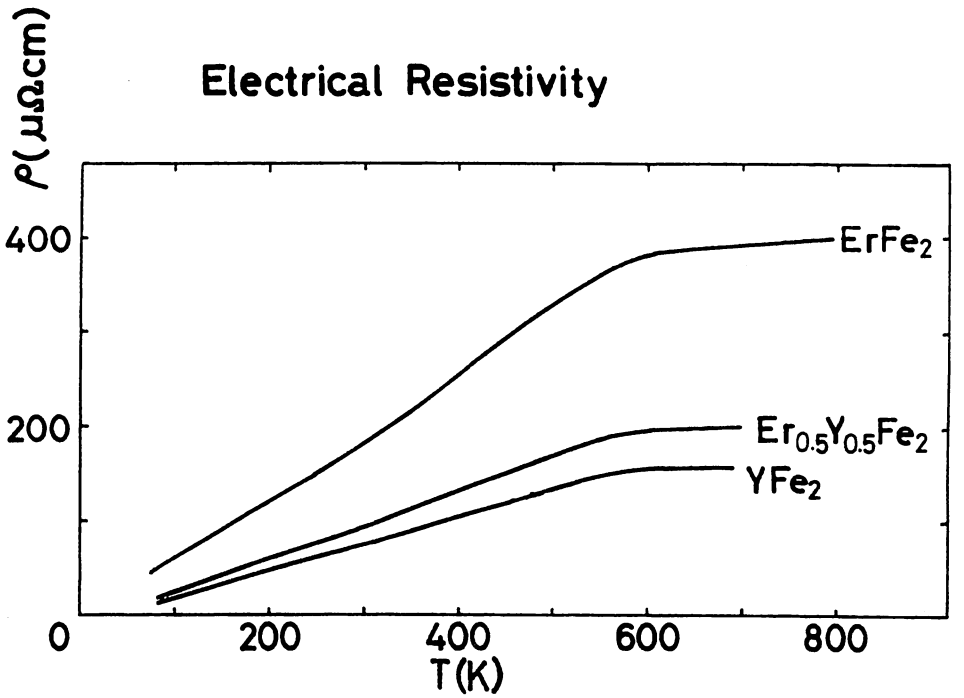

Fig.7; Temperature dependence of resistivity for $Er_{1-x}Y_xFe_2$.

Electrical resistivity ρ may be expressed as the sum of ρ_{im} due to impurity scattering, ρ_m due to magnetic scattering, and ρ_{ph} due to phonon scattering (Matthiessen's law). ρ_{im} can be obtained as the linear extrapolation to 0K, because it is independent of temperature. ρ_{im} is negligible for all specimens. Temperature dependence below T_c is due mainly to ρ_m. ρ_m saturates at T_c where atomic moments are in disorder. Therefore, ρ_m is a constant above T_c. Linear increase above T_c is due to the fact that ρ_{ph} increases linearly with increasing temperature. Gradients of the curves above T_c are almost the same for all the specimens. Therefore, as we can conclude that ρ_{ph} is independent of x, the states of conduction electrons are almost the same for all the spacimens.

We cam obtain ρ_m subtracting ρ_{ph} from ρ. ρ_m decreases with increasing x. Because the number of Fe ion is independent of x, we may conclude that the decrease in ρ_m is due to the decrease in the number of Er ions.

d. Hall constants

In Fig.8, field dependence of Hall resistivity (ρ_H) at 295K and 400K is shown. ρ_H saturates above 10kOe as in the case of magnetization. Hall resistivity ρ_H is expressesd as the sum

of normal Hall resistivity ρ_{nor} and abnormal Hall resistivity ρ_{abnor}. ρ_{nor} is due to the Lorentz force which is active over the entire range of the magnetic field. In the case of one conduction band, ρ_{nor} is proportional to the field. ρ_{nor} may be obtained by drawing a line parallel to the linear part of the curve after the saturation of magnetization. ρ_{abnor} is due to the magnetic moments in the specimen and saturates as the magnetization saturates. Therefore, one can obtain ρ_{abnor} subtracting ρ_{nor} from ρ_H measured at any field.

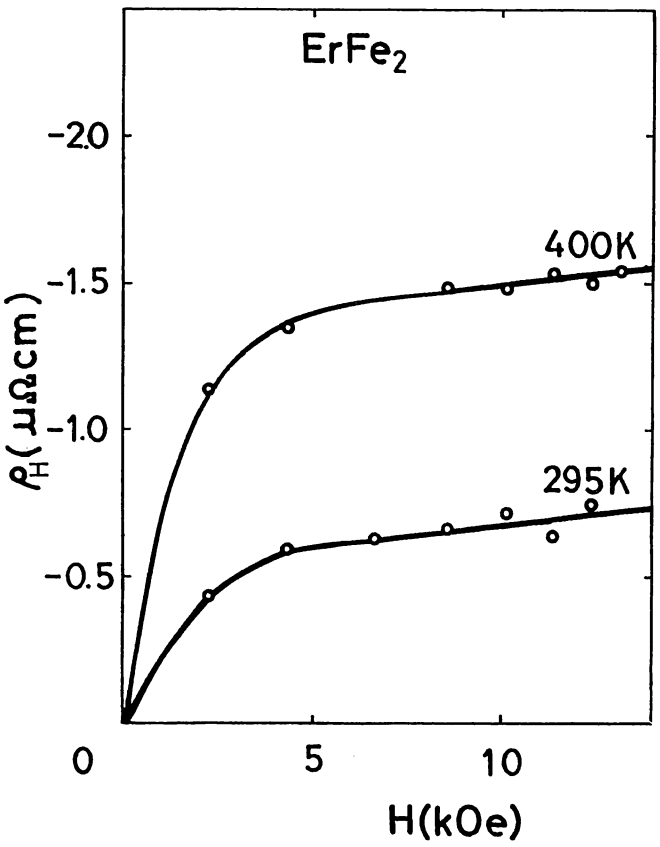

Fig.8; Field dependence of the Hall resistivity at 295K and 400K for $ErFe_2$.

By observation of Fig.8, we can find that ρ_{nor} is much smaller than ρ_{abnor} and almost independent of temperature. Thus Hall constants were measured at field 10kOe in order to investigate the temperature dependence of ρ_{abnor}.

In Fig.9, the temperature dependence of ρ_{abnor} is shown. ρ_{abnor} is maximum just below T_c for each specimen. ρ_{abnor} changes its sign around θ_c. ρ_{abnor} is positive and negative at temperatures above and below θ_c, respectively. The obtained Hall resisivity is essentially the same as that obtained by Hiraoka[4].

Results of measurement and calculation discussed in detail in § 4 are given in Table I.

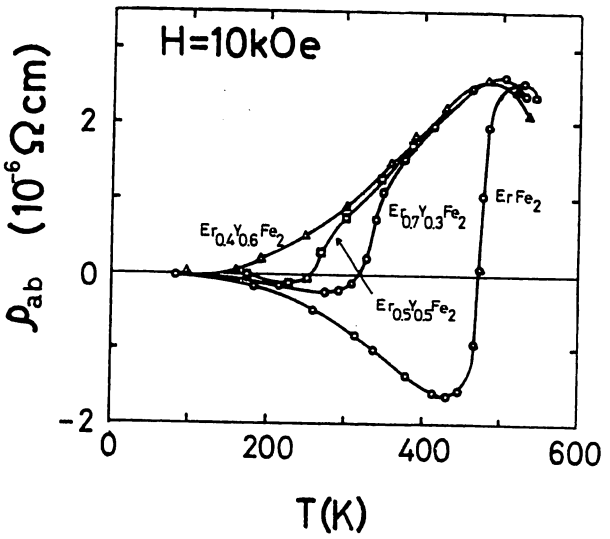

Fig.9; Temperature dependence of anomalous Hall resistivity at H=10kOe.

$Er_{1-x}Y_xEe_2$

x	0	0.3	0.4	0.5	0.6	1.0	単位
T_C	590	576	571	566	562	544	K
θ_C	468	317	268	246	139	—	K
A_0	7.282	7.306	7.314	7.322	7.331	7.356	Å
$m_{Fe}(0)$	2.15	1.71	1.66	1.63	1.59	1.43	
$m_{Er}(0)$	9	9	9	9	9	9	
n_{Fe}	16	16	16	16	16	16	
n_{Er}	8.0	5.6	4.2	4.0	3.2	0	
N_{Fe-Fe}	-4126	-7163	-7661	-7941	-8472	-10623	G^2cm^2/erg
N_{Er-Fe}	976	931	923	900	887	—	G^2cm^2/erg
N_{Er-Er}	-50	-140	-460	-490	-400	—	G^2cm^2/erg
C_1	2.342	5.647	—	—	7.554	—	
C_2	-9.120	-2.199	—	—	-1.786	—	$\times10^{-3}$
D_1	34.64	—	—	66.58	—	376.8	
D_2	16.26	—	—	7.180	—	—	

Table 1; Physical properties of $Er_{1-x}Y_xFe_2$. T_C denotes Curie temperature, θ_C, compensation temperature, A_0, lattice constant, m, atomic magnetic-moment in Bohr magnetons, n, number of atoms in a unit cell, and N, molecular field constant, where suffixes Fe and Er mean Fe sublattice and Er sublattice, respectively. C_1 and C_2 are contribution factor for the anomalous Hall resistivity from Fe and Er sublattices, respectively. D_1 and D_2 are contribution factor for the electrical resistivity from the Fe and Er sublattices, respectively.

§ 4. Discussion

1−a. Magnetization

As the result of magnetization measurement, it was assumed that both of the Fe and Er moments couple ferromagnetically themselves, and Fe and Er moments couple antiferromagnetically. To verify the assumption and to clarify the interaction between magnetic moments, magnetization curves were analyzed in terms of molecular field approximation[5].

There are Fe and Er sublattices in this system. N_{Fe-Fe} is the molecular field constant for the field on the Fe moments due to Fe sublattice. N_{Er-Er} is the molecular field constant for the field on Er moments due to Er sublattice. N_{Fe-Fe} and N_{Er-Er} are positive. N_{Fe-Er} is the molecular field constant for the field on Fe due to Er and vice versa and is positive. These three molecular field constants are taken into account in the process of molecular field analysis. Magnetic moments are distributed among the energy levels in proportion to the Boltzmann factor. One can calculate the magnetization using the Brillouin function.

Let the magnetization moments per atom of Fe and Er at absolute temperature T be $M_{Fe}(T)$ and $M_{Er}(T)$, respectively, which are transformed as follows,

$$M_{Fe}(T)=m_{Fe}(T)\mu_B,\ M_{Er}(T)=m_{Er}(T)\mu_B.$$

μ_B is the Bohr magneton.

$$m_{Fe}(T)=m_{Fe}(0)B_{1/2}(x_{Fe}) \tag{1}$$

$$m_{Er}(T)=m_{Er}(0)B_{15/2}(x_{Er}) \tag{2}$$

$B_{1/2}$ and $B_{15/2}$ are the Brillouin functions for $J=1/2$ and $J=15/2$. $m_{Fe}(0)$ and $m_{Er}(0)$ are the Bohr magneton numbers at 0K of Fe and Er ions, respectively. Theoretical value for Er^{3+} ion is $g_{Er}J_{Er}=9$, which agree with experimental value closely. We referred Buschow et al.[3] for $m_{Fe}(0)$. $B_{1/2}$ is used, because the magnetization curve of Fe at high temperature is well described by this function.

Variables in the Brillouin functions, x_{Fe} x_{Er} are expressed in terms of the molecular fields due to the sublattice, as follows

$$x_{Fe}=M_{Fe}(0)/kT-N_{Fe-Fe}I_{Fe}(T)+N_{Fe-Er}I_{Er}(T)$$

$$x_{Er}=M_{Er}(0)/kT+N_{Fe-Er}I_{Fe}(t)-N_{Er-Er}I_{Er}(T).$$

These equations can be rewritten

$$x_{Fe}=\mu_B^2 m_{Fe}(0)/ka_0^3 T\{-N_{Fe-Er}n_{Fe}m_{Fe}(T)+N_{Fe-Er}m_{Er}(T)\} \tag{3}$$

$$x_{Er}=\mu_B^2 m_{Er}(0)/ka_0^3 T\{\ N_{Fe-Er}n_{Fe}m_{Fe}(T)-N_{Er-Er}m_{Er}(T)\} \tag{4}$$

$I_{Fe}(T)$ and $I_{Er}(T)$ are the magnetization of Fe and Er sublattice at temperature T, respectively. n_{Fe} and n_{Er} are the number of Fe and Er ions in a unit cell. a_0 is the lattice constant. k is the Boltzmann's constant. It is difficult to solve equations (3) and (4) for the molecular field constants analytically. We tried to solve it graphically.

1−b. Determination of the molecular field constants

Absolute values of the magnetization of the sublattices are equal at the compensation temperature $\theta_C(T=\theta_C)$.

$$n_{Fe}m_{Fe}(\theta_C)=n_{Er}m_{Er}(\theta_C)=m_C(\theta_C) \quad (5)$$

Equations (3) and (4) can be rewritten as,

$$x_{Fe}=m_{Fe}(0)Q\{-N_{Fe-Fe}+N_{Fe-Er}m_C(\theta_C)\} \quad (6)$$

$$x_{Er}=m_{Er}(0)Q\{\ N_{Fe-Er}-N_{Er-Er}m_C(\theta_C)\} \quad (7)$$

where,

$$Q=\mu_B{}^2/(a_0{}^3\theta_C) \quad (8)$$

Equations (1), (2), (6) and (7) lead us to following equations.

$$m_C(\theta_C)=n_{Fe}m_{Fe}(0)B_{1/2}(x_{Fe}) \quad (9)$$

$$m_C(\theta_C)=x_{Fe}/m_{Fe}(0)Q(-N_{Fe-Fe}+N_{Fe-Er}) \quad (10)$$

$$m_C(\theta_C)=n_{Er}(0)B_{15/2}(x_{Er}) \quad (11)$$

$$m_C(\theta_C)=x_{Er}/m_{Er}(0)Q(N_{Fe-Er}-N_{Er-Er}) \quad (12)$$

We need to solve these equations graphically for $m_{Fe}(T)$, $m_{Er}(T)$, x_{Fe} and x_{Er}. Then the resultant magnetization must be equal to $m_C(\theta_C)$.

Magnetizations of both sublattices are not zero at the Curie temperature T_C. All the curves corresponding to the equations (9)−(12) cross the origin. Then the gradients of straight lines (10) and (12) give corresponding Brillouin functions. Gradients of the Brillouin functions $B_{1/2}$ and $B_{15/2}$ are obtained as follows,

$$B_{1/2}(x_{Fe})=(3J_{Fe}+1)x_{Fe}/3J_{Fe}$$

$$x_{Fe}=3J_{Fe}/(3J_{Fe}+1)B_{1/2}(x_{Fe}) \quad (13)$$

$$B_{15/2}(x_{Fe})=(3J_{Er}+1)x_{Er}/3J_{Er}$$

$$x_{Er}=3J_{Er}/(3J_{Er}+1)B_{15/2}(x_{Er}) \quad (14)$$

$B_{1/2}$ is used for Fe ions but the magnetic moment of the ions is larger than $1\,\mu_B$ for the state $J=1/2$, we introduce the multiple factor α: Fe moment is α times larger than that for $J=1/2$,

$$m_{Fe}(0)=g_{Fe}(\alpha) \quad (15)$$

values of α (or $m_{Fe}(0)$ are listed in the Table I.

Following expression for T_C may derived from the equations so far appeared.

$$T_C=-1/2(\alpha^2N_{Fe-Fe}C_{Fe}+N_{Er-Er}C_{Er})$$
$$+1/2\{(\alpha^2N_{Fe-Fe}C_{Fe}-N_{Er-Er}C_{Er})^2+4N_{Fe-Er}C_{Fe}C_{Er}\alpha^2\}^{1/2} \quad (16)$$

where,

$$C_{Fe}=g_{Fe}{}^2J_{Fe}(J_{Fe}+1)\mu_B{}^2n_{Fe}/3ka_0{}^3 \quad (17)$$

$$C_{Er}=g_{Er}{}^2J_{Er}(J_{Er}+1)\mu_B{}^2n_{Fe}/3ka_0{}^3 \quad (18)$$

We derived five equations (9), (10), (11), (12) and (16). But there are six variables, $m_C(\theta_C)$, x_{Fe}, x_{Er}, N_{Fe-Fe}, N_{Fe-Er}, and N_{Er-Er}, to be determined. We can not determine the molecular field coefficients uniquely. There is another condition that the molecular field coefficients should satisfy. Every molecular coefficient $Er_{1-x}Y_xFe_2$ should coincide with that of YFe_2 smoothly. N_{Fe-Fe} can be obtained from equation (18).

Thus obtained molecular field coefficients are shown in Fig.10. Absolute value of N_{Fe-Fe} increses linearly with increasing x. $ErFe_2$ seems to be exceptional. This fact suggests that the moment of $ErFe_2$ is exceedingly different from that of the other specimens. N_{Fe-Er} is respon-

sible for the ferrimagnetic arrangement of the magnetic moments. Absolute value of N_{Er-Er} increases with increasing x. This means the field at the site of Er ion due to surrounding Er moments increases with increasing x. Lattice constant increses with increasing x. Larger lattice constant reduces overlapping of $3d$ orbitals on the neighboring ions. Consequently, the direct interaction between Fe ions and the number of magnetic ions in an unit cell will be reduced. These effects will reduce the Curie temperature. The results of our reasoning agree with the experiment.

As a whole, the molecular constants obtained describe the magnetization of the system considered.

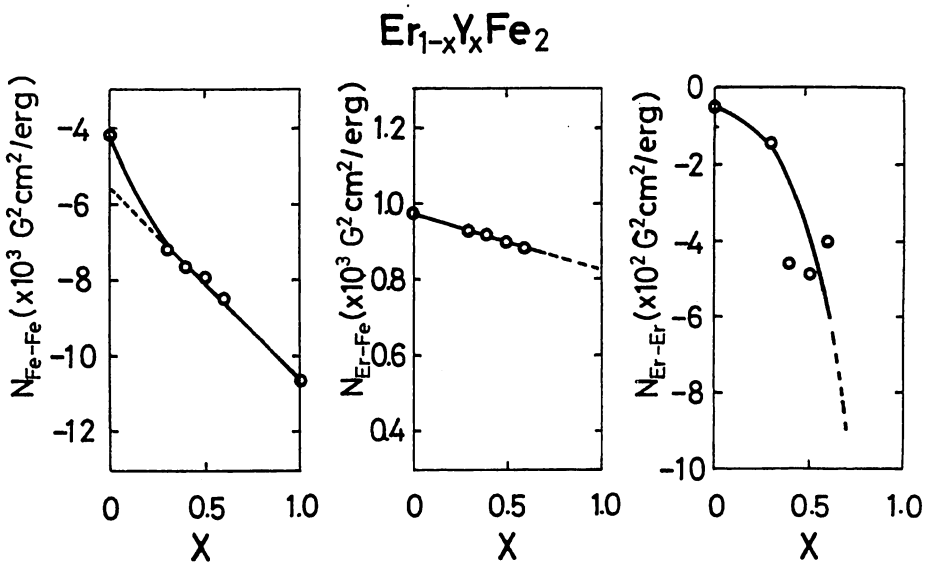

Fig.10; Molecular field coefficients.

1−c. Temperature dependence of the magnetization

Temperature dependence of the magnetization is described by using the molecular field constants thus obtained. Let the magnetic moment of Er per unit cell is β times that of Fe.

$$n_{Er} m_{Er}(T) = \beta\, n_{Fe} m_{Fe}(T) \tag{19}$$

Substituting (19) into (3) and (4), we get

$$x_{Fe} = m_{Fe}(0) P / T \{ -N_{Fe-FE} + \beta N_{Fe-Er} \}\, n_{Fe} m_{Fe}(T) \tag{20}$$

$$x_{Er} = m_{Er}(0) P / T \{ \quad N_{Fe-Er} - \beta N_{Er-Er} \}\, n_{Fe} m_{Fe}(T) \tag{21}$$

where, $P = \mu_B{}^2 / k a_0$

$$x_{Er} / x_{Fe} = m_{Er}(0) (N_{Fe-Er} - \alpha N_{Er-Er}) / m_{Fe}(0) (-N_{Fe-Fe} + \beta N_{Fe-Er}) = \gamma \tag{22}$$

γ will be determined uniquely when β is given.

Solving these equations graphically, we get the magnetization of the sublattices as a function of temperature. Temperature dependence of the sublattices are shown in Figs.11−16. Solid line, broken line, and dotted line represent the total moment of Er and Fe, the moment of Er sublattice and the moment of Fe sublattice, respectively. Experimental values are shown by open circles. Experimental results and the calculated values are brought into coincidence

at 80K. Calculated magnetization follows closely the temperature dependence of the magnetization. Discrepancy between the calculated magnetization and the experimental results seems to increase with increasing x. This fact suggests that fluctuation, which increases with increasing x, thereby increasing the discrepancy, in composition and in the crystal field will be present in these polycrystals used in this experiment.

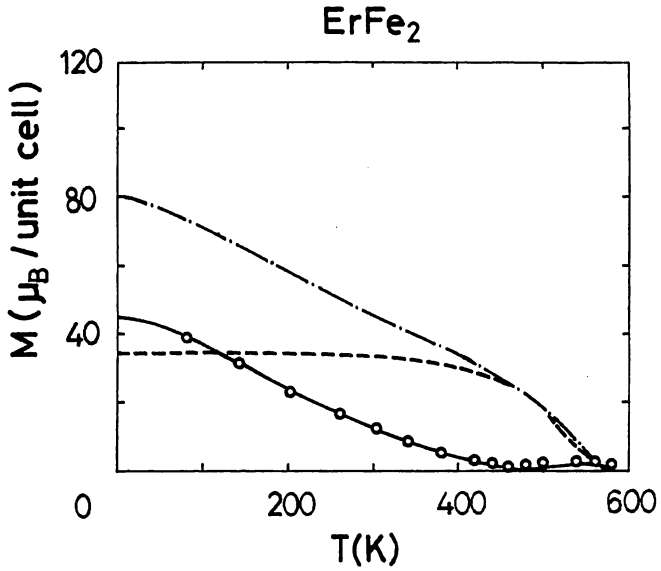

Fig.11; Calculated temperature dependence for the magnetic moment of Fe and Er sublattices and the total magnetic moments. ——: total moments, - - - -: Fe sublattice moments, and —·—: Er sublattice moments. o's are the experimental values for $ErFe_2$.

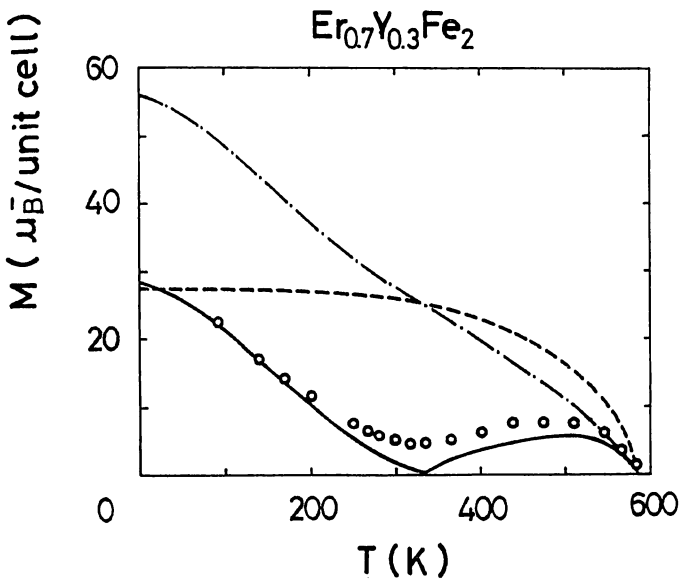

Fig.12; For $Er_{0.7}Y_{0.3}Fe_2$.

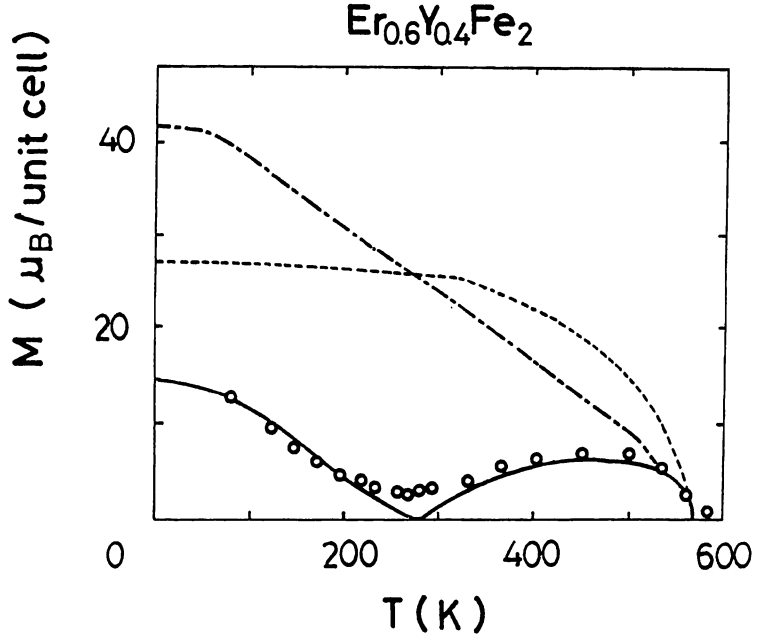

Fig.13; For $Er_{0.6}Y_{0.4}Fe_2$.

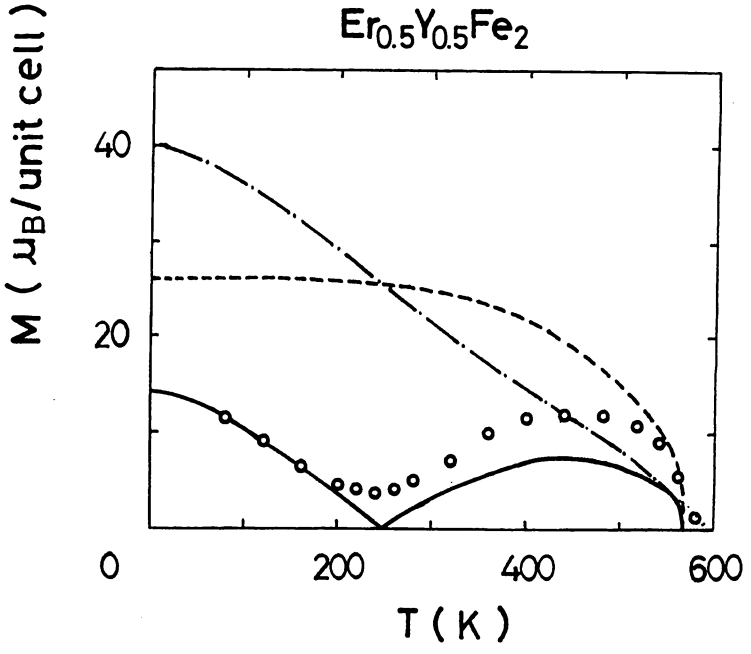

Fig.14; For $Er_{0.5}Y_{0.5}Fe_2$.

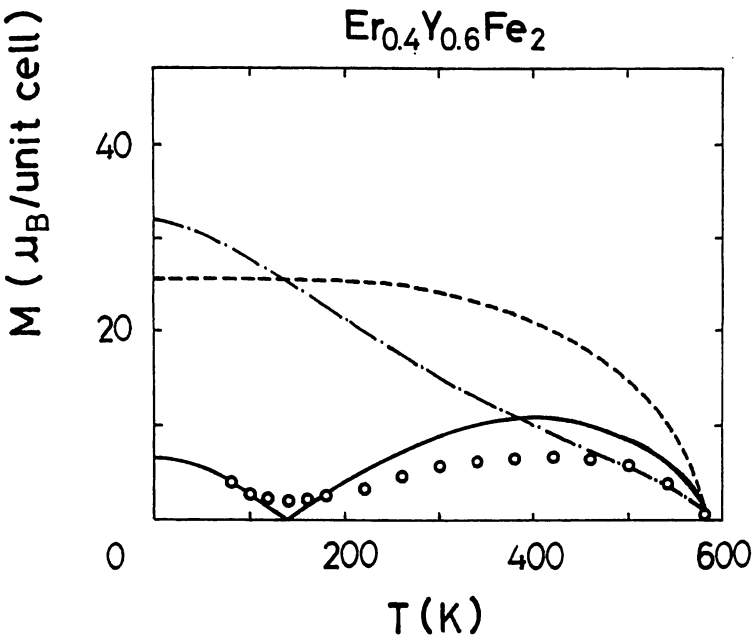

Fig.15; For $Er_{0.4}Y_{0.6}Fe_2$.

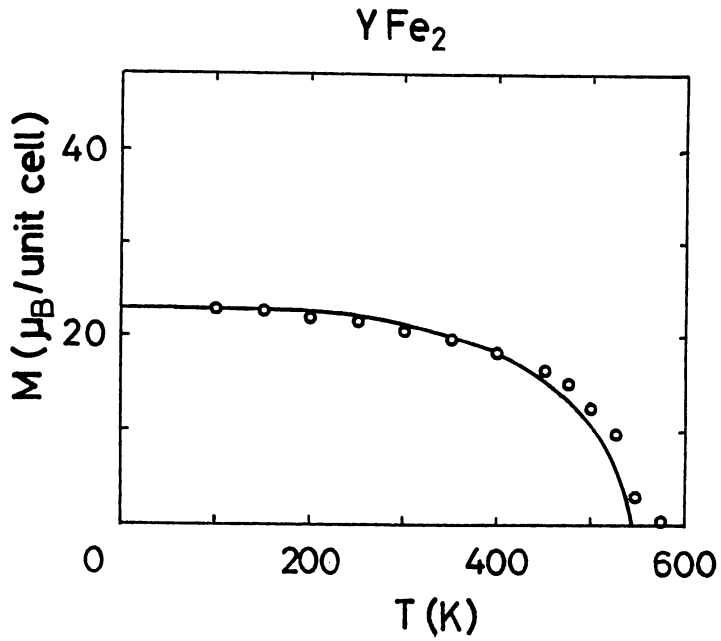

Fig.16; Temperature dependence of magnetization for YFe_2.

2. Electrical Resistivity

In this subsection, we discuss how the conduction electrons are scattered by moments in Er and Fe sublattices. The band structure is considered to be rigid, because $\Delta\rho_{ph}/\Delta T$ is almost constant over the whole range of x. Rare earths are well described by a localized moment model. Fe is believed to have comparatively strong character of localized moment. Our discussion will be based on the localized model.

Kasuya [6] caluculated ρ_m with following supposition.[1] Magnetic moments are lacalized. They scatter the conduction electrons but they do not contribute to conduction themselves.[2] The only carriers are s electrons (1-band model).[3] Interaction between localized and conduction electrons is spin-spin coupling.

A result of their caluculation is,

$$\rho_m \propto \langle (M_z - \langle M_z \rangle)^2 \rangle \tag{23}$$

where M is the magnetization. Electric resistivity is proportional to the average of squared fluctuation of the magnetization. (22) is applied to the sublattices.

$$\langle M_{Fez}^n \rangle \; \Sigma M_z^n \exp(M_z x_{Fe}/M, / \; \Sigma \exp(M_z x_{Fe}/M) \tag{24}$$

$M_z/M x_{Fe}$ is the potential energy of the moment M_z in the molecular field, which is along z-axis, devided by themal energy kT.

ρ_m may be described as the sum of contribution from the two sublattices.

$$\rho_m = D_1 \langle (M_{Fez} - \langle M_{Fez} \rangle)^2 \rangle + D_2 \langle (M_{Erz} - \langle M_{Erz} \rangle)^2 \rangle \tag{25}$$

where D_1 and D_2 are constants depending on the intensity of interaction. Fig.17 shows $\langle (M_{Fez} - \langle M_{Fez} \rangle)^2 \rangle$ and $\langle (M_{Erz} - \langle M_{Erz} \rangle)^2 \rangle$, in the case of $Er_{0.5}Y_{0.5}Fe_2$, caluculated on the basis of the temperature dependence of the sublattice magnetization obtained in the preceding section. D_1 and D_2 are determined so that (24) describes the experimental results most closely.

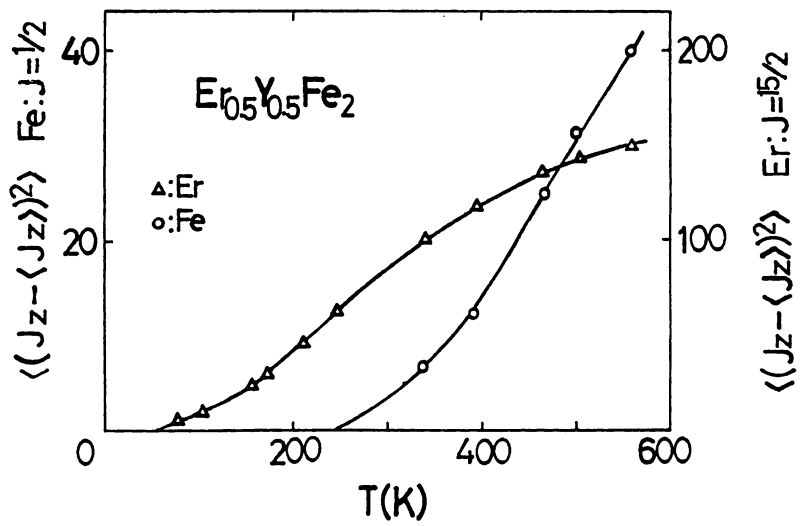

Fig.17; Calculated values for the mean squared fluctuation of the magnetic moments.

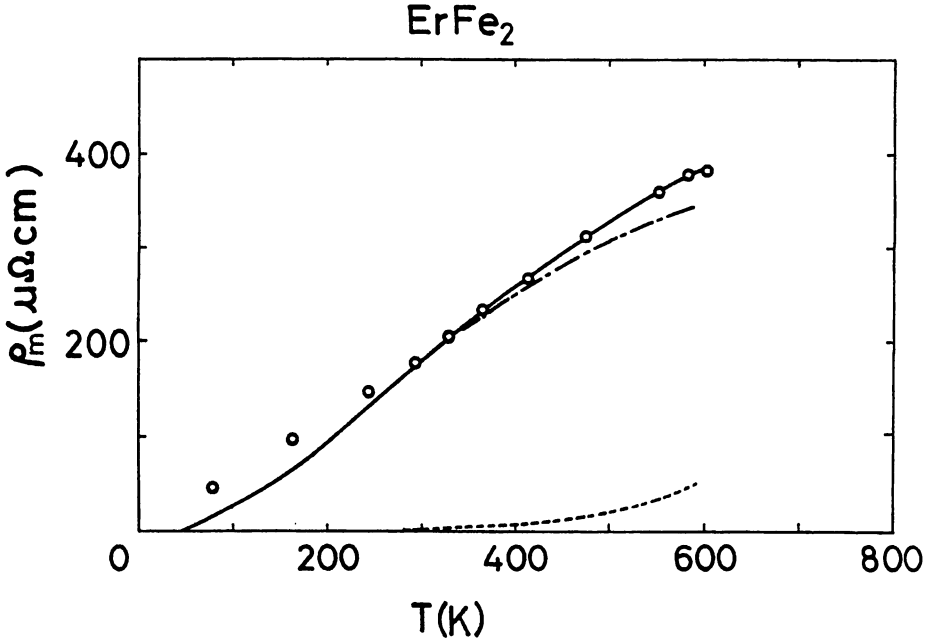

Fig.18; Calculated magnetic resistivity. ——: total, -----: Fe sublattice and —·—: Er sublattice. o's are experimental ones for $ErFe_2$.

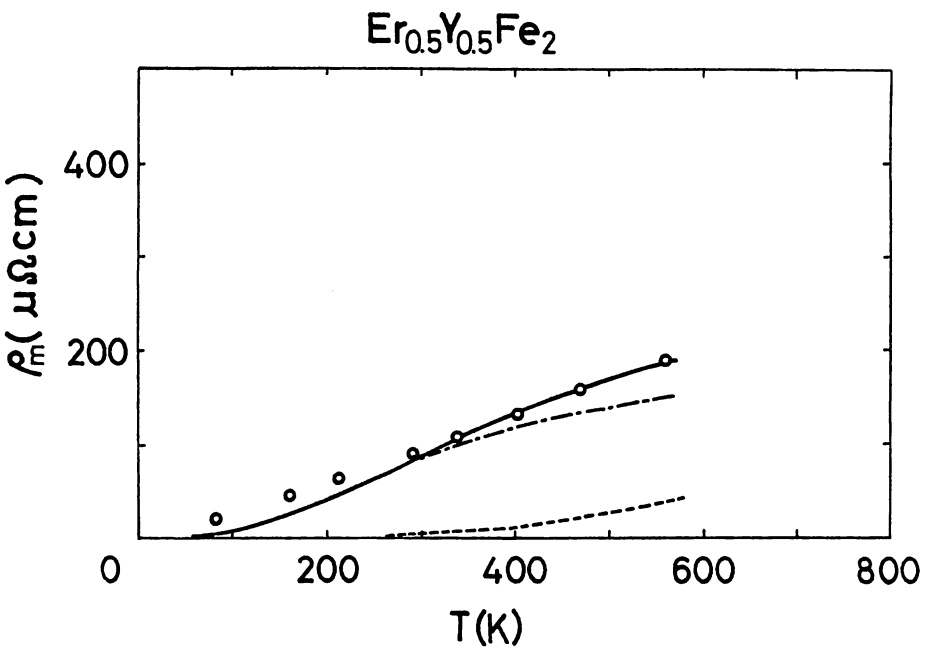

Fig.19; Calculated and experimental magnetic resistivity for $Er_{0.5}Fe_{0.5}$.

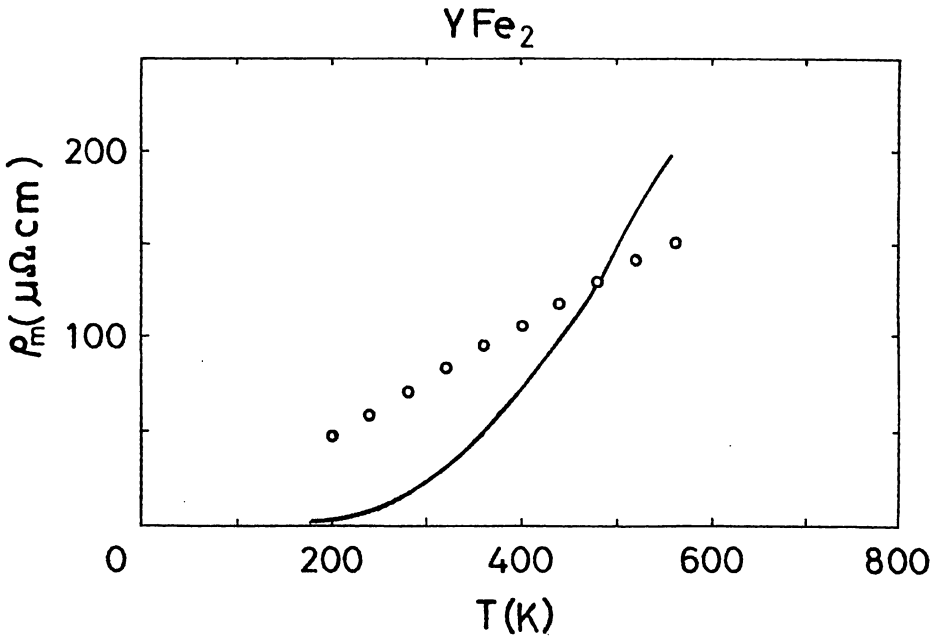

Fig.20; Calculated and Experimental magnetic resistivity for YFe_2.

In Figs.18, 19, 20, results of the analysis are shown. Contribution from the Er sublattice is much lagrger than that from the Fe sublattice. This may be the reflection of the fact that rare earths have much larger ρ_m than Fe. Agreement between the calculated and experimental values is better in the high temperature region than in the low temperature region. The agreement is better in the Er rich region than in the relatively Fe rich region. In the Fe rich region, localized model will not be valid and consequently the molecular field approximation used in this discussion will not be valid also. The large discrepancy between experimental and calculated results in YFe_2 supports this reasoning.

In general, magnetic properties are not described in terms of the molecular field approximation in the low temperature region. Spin wave models are used in low temperature region. Temperature dependence of the molecular field constant of Er sublattice shows that the molecular field approximation is applicable to rather low temperature. But the molecular field model is not good approximation in the case of Fe sublattice. Spin wave models may be applied to Fe sublattice, where $S-s$ coupling should also be included.

3. *Hall Effects*

The Hall resistivity changes its sign at compensation temperature θ_C. Magnetization of the sublattices are equal at θ_C. Below θ_C Er sublattice has larger magnetization than the Fe sublattice. At temperatures higher than θ_C the moment of Fe sublattice is larger than that of Er sublattice. Direction of the net magnetization changes at θ_C. Change of sign in ρ_H at θ_C is considered to be caused by this change in the direction of the spontaneous magnetization. Matthiessen's rule can be applied for ρ_H as in the case of electrical resistivity.

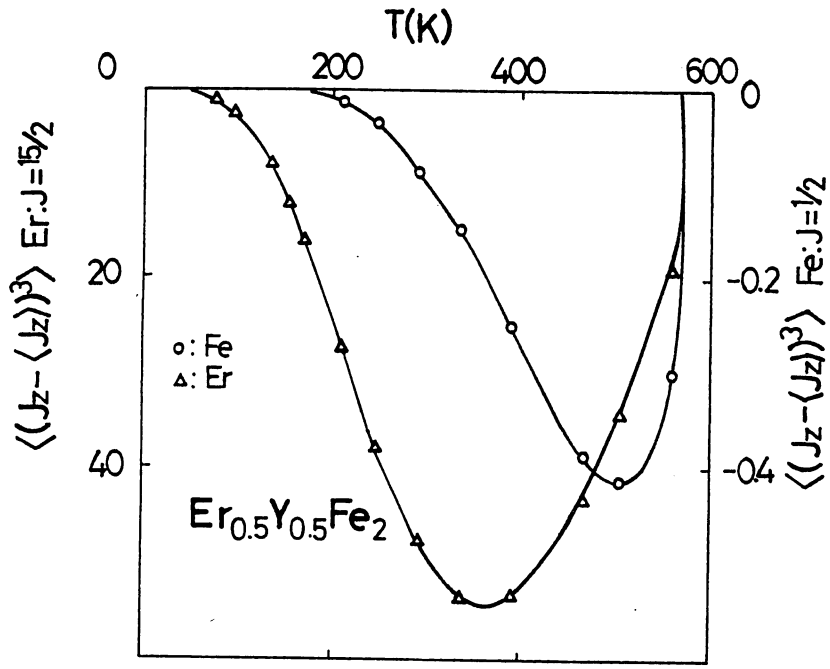

Fig.21; Calculated mean cubic fluctuation of the moments.

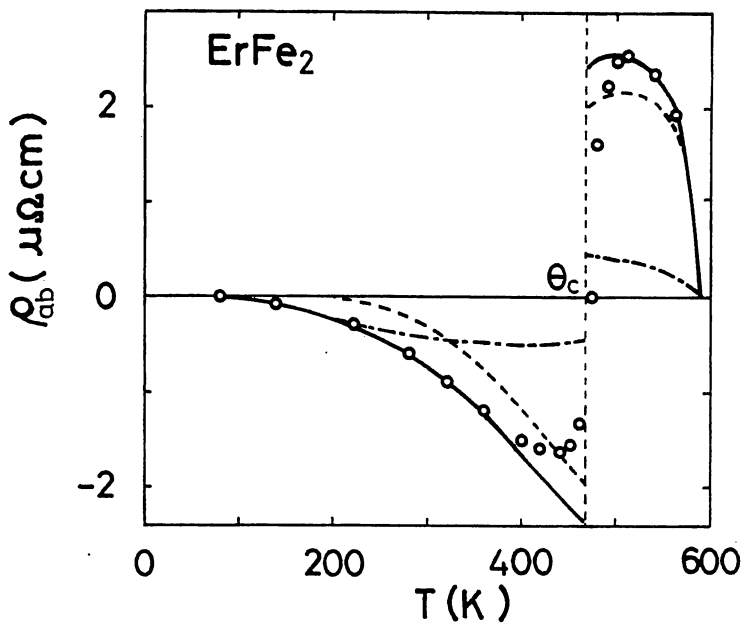

Fig.22; Calculated anomalous Hall resistivity. ——: total. ------: Fe sublattice, —·—: Er sublattice. o's are experimental ones for $ErFe_2$.

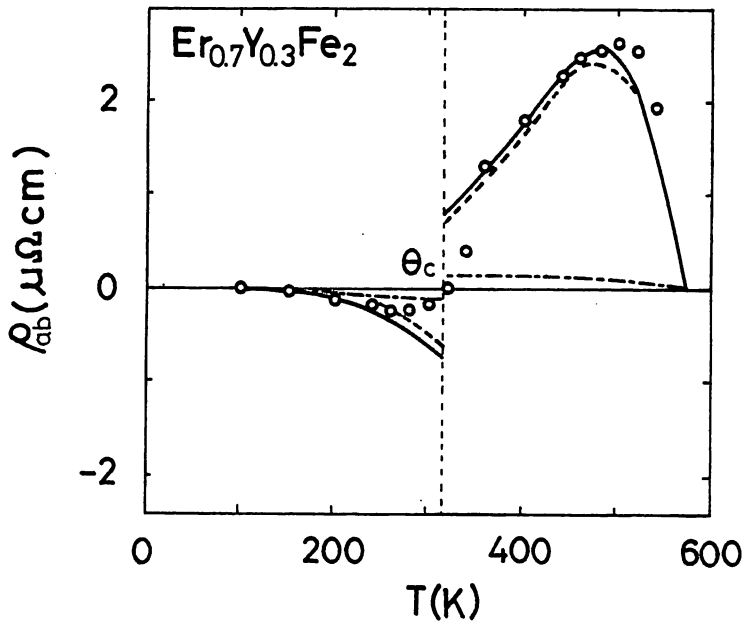

Fig.23; Calculated and experimental anomalous Hall resistivity for $Er_{0.7}Y_{0.3}Fe_2$.

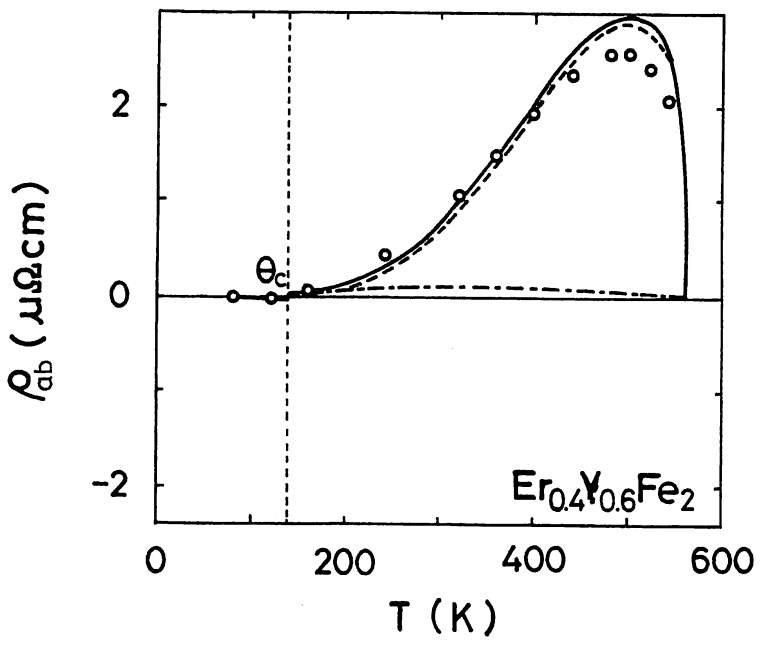

Fig.24; Calculated and experimental anomalous Hall resistivity for $Er_{0.4}Y_{0.6}Fe_2$.

We discuss the contributions to ρ_H from Er and Fe sublattices. Results of Maranzana's[7] and Kondo's[8] calculation, which are based on the localized moment model, are used. According to them, ρ_H is expressed as follows

$$\rho_H \langle (M - \langle M \rangle)^3 \rangle \tag{24}$$

Applying the Matthiessen's rule, ρ_H can be expressed as follows,

$$\rho_H = C_1 \langle (J_{Fez} - \langle J_{Fez} \rangle)^3 \rangle + C_2 \langle (J_{Erz} - \langle J_{Erz} \rangle)^3 \rangle \tag{25}$$

C_1 and C_2 depends on the intensity of the interaction. In Fig.21 shows temperature dependence of $\langle (J - \langle J \rangle)^3 \rangle$ for Er and Fe sublattice in the case of $Er_{0.5}Y_{0.5}Fe_2$. Values of C_1 and C_2, determined as in the case of D_1 and D_2, for several x are listed in Table I. Results of calculation are shown in Figs.22,23 and 24. Results are shown in reversed way at the compensation temperature θ_C as the net magnetization changes its direction at this temperature. Agreement between experimental and calculated ρ_H is good for the specimens shown. Comparing the results of electrical resistivity and Hall resistivity, we can conclude that the localized model based on the molecular field approximation is more suited for Hall resistivity than for electrical resistivity.

As a whole, we can describe magnetic and galvanomagnetic properties of this system in terms of the localized model based on the molecular field approximation. It is remarked that even thought the magnetization and the Hall resistivity are described by localized model, the electrical resistivity is not amenable to this model for Fe. Band structure and spin wave model should be adopted for further analysis.

References

1) N. Takuro, *Kotai Butsuri* (in Japanese), **9**, No.12, (1974)
2) Rodney P. Elliott, Ph. D
   "*Constitution of Binary Alloys*" p.442 (MacGrow− Hill, 1965)
3) K. H. J. Buschow and R. P. van Stapele,
   J. Appl. Phys. **41** No. 10, 4060 (1970)
4) T. Hiraoka, J. Phys. Soc. Jpn., **49** 2195 (1980)
5) Allan H. Morrish,
   "*The Principles of Magnetism*" p.490 (Robert E. Krieger, 1980)
6) T. Kasuya, Prog. Theor. Phys., **16** 1 (1956)
7) F. E. Maranzana, Phys. Rev., **160** 2 (1967)
8) J. Kondo, Prog. Theor. Phys., **27** 4 (1962)